REPORT DOCUMENTATION PAGE

Form Approved
OMB No. 0704-0188

1. AGENCY USE ONLY (*Leave blank*)	2. REPORT DATE	3. REPORT TYPE AND DATES COVERED
	May 2004	Technical Memorandum

4. TITLE AND SUBTITLE

Leakage and Power Loss Test Results for Competing Turbine Engine Seals

5. FUNDING NUMBERS

WBS–22–714–09–18
1L161102AF20

6. AUTHOR(S)

Margaret P. Proctor and Irebert R. Delgado

7. PERFORMING ORGANIZATION NAME(S) AND ADDRESS(ES)

National Aeronautics and Space Administration
John H. Glenn Research Center at Lewis Field
Cleveland, Ohio 44135–3191

8. PERFORMING ORGANIZATION REPORT NUMBER

E–14452

9. SPONSORING/MONITORING AGENCY NAME(S) AND ADDRESS(ES)

National Aeronautics and Space Administration
Washington, DC 20546–0001
and
U.S. Army Research Laboratory
Adelphi, Maryland 20783–1145

10. SPONSORING/MONITORING AGENCY REPORT NUMBER

NASA TM—2004-213049
ARL–TR–3157
GT2004–53935

11. SUPPLEMENTARY NOTES

Prepared for the Turbo Expo 2004 sponsored by the American Society of Mechanical Engineers, Vienna, Austria, June 14–17, 2004. Margaret P. Proctor, NASA Glenn Research Center; and Irebert R. Delgado, U.S. Army Research Laboratory, NASA Glenn Research Center. Responsible person, Margaret P. Proctor, organization code 5950, 216–977–7526.

12a. DISTRIBUTION/AVAILABILITY STATEMENT

Unclassified - Unlimited
Subject Category: 07 Distribution: Nonstandard

Available electronically at http://gltrs.grc.nasa.gov

This publication is available from the NASA Center for AeroSpace Information, 301–621–0390.

12b. DISTRIBUTION CODE

13. ABSTRACT ***(Maximum 200 words)***

Advanced brush and finger seal technologies offer reduced leakage rates over conventional labyrinth seals used in gas turbine engines. To address engine manufacturers' concerns about the heat generation and power loss from these contacting seals, brush, finger, and labyrinth seals were tested in the NASA High Speed, High Temperature Turbine Seal Test Rig. Leakage and power loss test results are compared for these competing seals for operating conditions up to 922 K (1200 °F) inlet air temperature, 517 KPa (75 psid) across the seal, and surface velocities up to 366 m/s (1200 ft/s).

14. SUBJECT TERMS

Seals; Brush seal; Finger seal; Labyrinth seal; Leakage; Power loss; Performance

15. NUMBER OF PAGES

17

16. PRICE CODE

17. SECURITY CLASSIFICATION OF REPORT	18. SECURITY CLASSIFICATION OF THIS PAGE	19. SECURITY CLASSIFICATION OF ABSTRACT	20. LIMITATION OF ABSTRACT
Unclassified	Unclassified	Unclassified	

NASA/TM—2004-213049

ARL–TR–3157
GT2004–53935

Leakage and Power Loss Test Results for Competing Turbine Engine Seals

Margaret P. Proctor
Glenn Research Center, Cleveland, Ohio

Irebert R. Delgado
U.S. Army Research Laboratory, Glenn Research Center, Cleveland, Ohio

May 2004

The NASA STI Program Office . . . in Profile

Since its founding, NASA has been dedicated to the advancement of aeronautics and space science. The NASA Scientific and Technical Information (STI) Program Office plays a key part in helping NASA maintain this important role.

The NASA STI Program Office is operated by Langley Research Center, the Lead Center for NASA's scientific and technical information. The NASA STI Program Office provides access to the NASA STI Database, the largest collection of aeronautical and space science STI in the world. The Program Office is also NASA's institutional mechanism for disseminating the results of its research and development activities. These results are published by NASA in the NASA STI Report Series, which includes the following report types:

- TECHNICAL PUBLICATION. Reports of completed research or a major significant phase of research that present the results of NASA programs and include extensive data or theoretical analysis. Includes compilations of significant scientific and technical data and information deemed to be of continuing reference value. NASA's counterpart of peer-reviewed formal professional papers but has less stringent limitations on manuscript length and extent of graphic presentations.

- TECHNICAL MEMORANDUM. Scientific and technical findings that are preliminary or of specialized interest, e.g., quick release reports, working papers, and bibliographies that contain minimal annotation. Does not contain extensive analysis.

- CONTRACTOR REPORT. Scientific and technical findings by NASA-sponsored contractors and grantees.

- CONFERENCE PUBLICATION. Collected papers from scientific and technical conferences, symposia, seminars, or other meetings sponsored or cosponsored by NASA.

- SPECIAL PUBLICATION. Scientific, technical, or historical information from NASA programs, projects, and missions, often concerned with subjects having substantial public interest.

- TECHNICAL TRANSLATION. English-language translations of foreign scientific and technical material pertinent to NASA's mission.

Specialized services that complement the STI Program Office's diverse offerings include creating custom thesauri, building customized databases, organizing and publishing research results . . . even providing videos.

For more information about the NASA STI Program Office, see the following:

- Access the NASA STI Program Home Page at ***http://www.sti.nasa.gov***

- E-mail your question via the Internet to help@sti.nasa.gov

- Fax your question to the NASA Access Help Desk at 301–621–0134

- Telephone the NASA Access Help Desk at 301–621–0390

- Write to:
  NASA Access Help Desk
  NASA Center for AeroSpace Information
  7121 Standard Drive
  Hanover, MD 21076

NASA/TM—2004-213049

ARL–TR–3157
GT2004–53935

Leakage and Power Loss Test Results for Competing Turbine Engine Seals

Margaret P. Proctor
Glenn Research Center, Cleveland, Ohio

Irebert R. Delgado
U.S. Army Research Laboratory, Glenn Research Center, Cleveland, Ohio

Prepared for the
Turbo Expo 2004
sponsored by the American Society of Mechanical Engineers
Vienna, Austria, June 14–17, 2004

National Aeronautics and
Space Administration

Glenn Research Center

May 2004

Acknowledgments

The authors acknowledge the contributions of Arun Kumar and his colleagues at Honeywell Engines, Systems & Services towards the development of the finger seal tested at NASA Glenn Research Center. The authors also acknowledge the contributions of the NASA Glenn Research Center at Lewis Field, Cleveland, Ohio where all testing was conducted, particularly the leadership of Dr. Bruce M. Steinetz who guided the design, procurement, and fabrication of the High Temperature, High Speed, Turbine Seal Test Rig.

Available from

NASA Center for Aerospace Information
7121 Standard Drive
Hanover, MD 21076

National Technical Information Service
5285 Port Royal Road
Springfield, VA 22100

Available electronically at http://gltrs.grc.nasa.gov

Leakage and Power Loss Test Results for Competing Turbine Engine Seals

Margaret P. Proctor
National Aeronautics and Space Administration
Glenn Research Center
Cleveland, Ohio 44135

Irebert R. Delgado
U.S. Army Research Laboratory
Glenn Research Center
Cleveland, Ohio 44135

ABSTRACT

Advanced brush and finger seal technologies offer reduced leakage rates over conventional labyrinth seals used in gas turbine engines. To address engine manufacturers' concerns about the heat generation and power loss from these contacting seals, brush, finger, and labyrinth seals were tested in the NASA High Speed, High Temperature Turbine Seal Test Rig. Leakage and power loss test results are compared for these competing seals for operating conditions up to 922 K (1200 °F) inlet air temperature, 517 KPa (75 psid) across the seal, and surface velocities up to 366 m/s (1200 ft/s).

INTRODUCTION

Reducing secondary air leakage within jet engines enables higher engine performance in terms of decreased specific fuel consumption and increased available thrust [1]. These reductions are made possible by the use of current and advanced engine seals, such as labyrinth, brush, or finger seals, which are used to control leakage across a stationary/rotating interface within a jet engine. Studies have shown that small investments in sealing technology have shown a greater increase in engine performance than investments made to improve component technologies such as compressors or turbines [1].

Heat generation and power loss effects through seal use are necessary considerations that can negatively impact engine performance. Changes in engine air temperatures from stage to stage can negatively affect engine efficiencies. For example, heat generation may cause unaccounted rotor or casing growth resulting in increased clearances, higher leakage rates, and reduced engine efficiencies [1]. Moreover, friction generated from contacting seals increases the amount of torque the rotating machinery needs to overcome to produce thrust thereby reducing the efficiency of the engine. Advanced engines operate at very high temperatures; and significant heat generation at the seals could expose downstream components to temperatures that exceed material capabilities.

Baseline labyrinth and brush seals were tested in NASA Glenn Research Center's High-Speed, High-Temperature Turbine Seal Test Rig. Static, performance, and endurance tests were conducted. The results of these baseline tests are compared to each other and to finger seal leakage and power loss performance data obtained in the same test rig. Brush and finger seal wear results are presented along with an assessment of the rotor coating performance.

NOMENCLATURE

A	=	contact area
D_{seal}	=	outside diameter of the test rotor, m
D_I	=	bearing bore diameter, m
P	=	contact pressure
P_{ower}	=	frictional seal power loss
P_u	=	air pressure upstream of seal, MPa
T	=	torque loss, N-m
T_{avg}	=	average seal air inlet temperature, K
U	=	surface velocity
W	=	load on bearing, N
f	=	friction coefficient
$\dot{m}$	=	air leakage flow rate, kg/s
μ	=	friction coefficient
ϕ	=	flow factor, kg-$\sqrt{K}$/MPa-m-s

TEST HARDWARE

Labyrinth Seal

Used for many years to control leakage across a stationary/rotating interface within jet engines, labyrinth seals are clearance seals composed of a number of axially spaced knife edges offset a distance from the opposing surface. A pressure drop, as exists between compressor or turbine stages within a jet engine, is present across the labyrinth seal due to its alternating series of knife edges and cavities which dissipates the kinetic energy of the fluid flowing through it [1]. However, the labyrinth seal's sealing capability is limited by the need to maintain a clearance from the rotating surface. This, in turn, limits the amount of leakage that can be controlled which affects the maximum engine performance.

The labyrinth seal used in this study, fig. 1, was designed using the KTK computer code [2] to predict its leakage performance. KTK calculates the leakage and pressure distribution through labyrinth seals based on a detailed knife-to-knife analysis. The labyrinth seal tested is

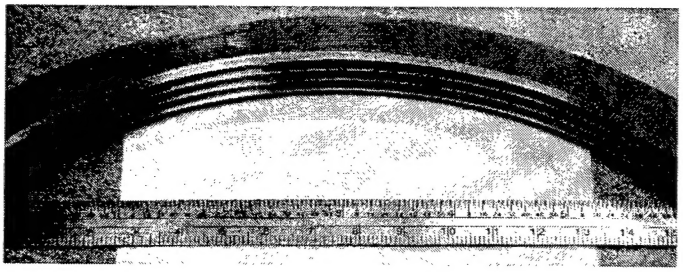

Figure 1.—Four-knife labyrinth seal made of Inconel 625.

a straight four-knife design with a nominal 229 μm radial clearance at assembly with the 215.9 mm diameter rotor. The 229 μm radial clearance is too small to ensure non-contacting operation at temperature and speed. Hence, only static room temperature tests were conducted. Key design features are given in table 1.

Table 1.—Labyrinth seal design parameters.

Material	Inconel 625
Type	straight
Number of knives	4
Rotor outer diameter	215.9 mm
Tooth height	2.286 mm
Tooth taper angle	7.5 degrees
Land thickness	305 μm
Tooth pitch	3.175 mm
Radial clearance	127 μm
Seal inner diameter	216.154 mm

Brush Seal

Brush seals are contacting seals composed of a dense pack of high-temperature alloy wires captured between stationary plates and pointed inward towards the rotating surface at an angle to the radius of the seal. They control leakage more effectively than labyrinth seals [3] because their compliant nature permits a smaller clearance to be used and the bristles track rotor radial growth due to rotation and temperature. However frictional heating due to contact with the rotating surface tends to quickly wear the brush seal and limit its useful life.

A commercially available brush seal (fig. 2) with a flow deflector was used for this study. It is composed of Inconel-625 sideplates and 102 μm diameter Haynes-25 bristles at a 50° angle to the radius. The bristle density at the seal inner diameter (id) is approximately 675 bristles/cm of circumference. The initial radial interference with the rotor was 96.5 μm. The fence height, the distance between the rotor and the downstream side plate, is 1.27 mm. The total axial thickness of the brush seal was 4.27 mm.

It should be noted that brush seal designs vary, and that brush seal leakage performance is strongly dependent on bristle pack stiffness and density, bristle angle, fence height, materials, etc. The brush seal tested is only one design and may or may not be the optimum for any aircraft engine application. It is, however, representative of typical brush seals used under the conditions at which the tests were conducted.

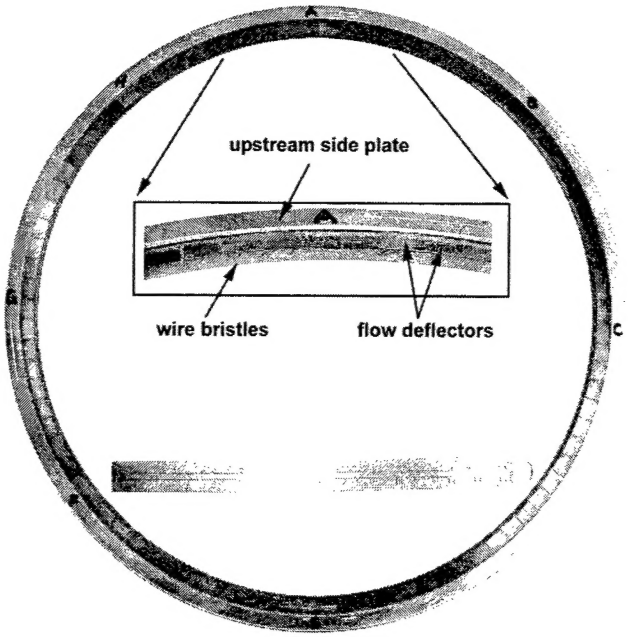

Figure 2.—Brush seal with flow deflector.

Finger Seal

In the mid to late 1990's a pressure balanced, low hysteresis finger seal was successfully developed and tested at NASA Glenn Research Center [4] and subsequently patented by AlliedSignal Engines [5]. In 2002 a 215.9 mm id pressure balanced finger seal was tested at inlet air temperatures up to 922 K, speeds up to 366 m/s, and pressure differentials up to 517 kPa [6]. Brush and labyrinth seal performance data are compared to this data. The finger seal, fig. 3, is composed of a series of finger elements sandwiched between aft and forward spacers and cover plates. Each finger element has been machined to create a series of slender curved beams or fingers around its inner diameter. The finger elements are alternately indexed so that the fingers of one element cover the spaces between the fingers on the adjacent element. The flexible fingers can bend radially to accommodate shaft excursions and relative growth of the seal and rotor resulting from rotational forces and thermal mismatch. The seal is made of sheet AMS5537, a cobalt-base alloy which has good formability, excellent high temperature properties, and displays excellent resistance to the hot corrosive atmospheres encountered in jet engine operations. The finger seal had an initial radial interference with the rotor of 165 μm.

Test Rotors

The test rotors used were nominally 215.9 mm in diameter and made of Grainex Mar-M-247. Their outer diameters were coated with chromium-carbide (CrC) applied with a high-velocity oxygen-fuel (HVOF) thermal spray process. The same rotor was used for the labyrinth and brush seals and had an inspected outer diameter (od) of 215.8975 mm. The rotor for the finger seal had an inspected od of 215.8949 mm.

TEST APPARATUS

Turbine Seal Test Rig

In the NASA High Temperature, High Speed Turbine Seal Test Rig, fig. 4, the 215.9 mm diameter test rotor is mounted on a shaft in an overhung configuration. The shaft is supported by two oil-lubricated bearings. A balance piston controls the axial thrust load on the bearings due to pressure loads on the test rotor. An air turbine drives the test rig. A torquemeter is located between the air turbine and the test rig and is connected to each by a quill shaft. The test seal is clamped into the Grainex Mar-M 247 seal holder as shown in figure 5. A C-seal located at the seal holder/test seal interface prevents flow from bypassing the test seal at its outer diameter. The seal holder is heated to approximately match the thermal growth of the rotor and to prevent a change in radial clearance that may damage the seal and/or rotor. Heated, filtered air enters the bottom of the test rig and passes through an inlet plenum that directs the heated air axially toward the seal–rotor interface. The hot air either leaks through the test seal to the seal exhaust line or exits the rig before the test seal through a controlled bypass line at the top of the rig. If seal leakage is low, the bypass line must be open to maintain sufficient flow through the test rig to keep the rig hot.

Instrumentation

Seal inlet and exit temperatures and static pressures, seal upstream metal temperature (finger seal only), and seal backface temperatures were measured at the locations shown in figure 5. For each measurement there were 3 probes equally spaced around the circumference, except for the upstream seal metal temperature for which 2 thermocouples were located at the 90° and 180° positions (0° is top-dead-center). Type-K thermocouples were used and all were 157 μm, Inconel sheath, closed ball except the seal exit temperatures, which were 3.2 mm diameter and the seal metal and backface temperatures, which were open-ball.

High temperature capacitance proximity probes were mounted in the seal holder at four equally-spaced locations to view the test rotor outer diameter. These probes were used to measure the change in clearance between the seal holder and the rotor and to monitor the rotordynamic behavior of the test rotor. The average inlet air temperature is used as the probe temperature when correcting the probe output. These proximity probes have an accuracy of 5 μm at room temperature. Proximity probe data were only available for some of the finger seal tests due to instrumentation problems.

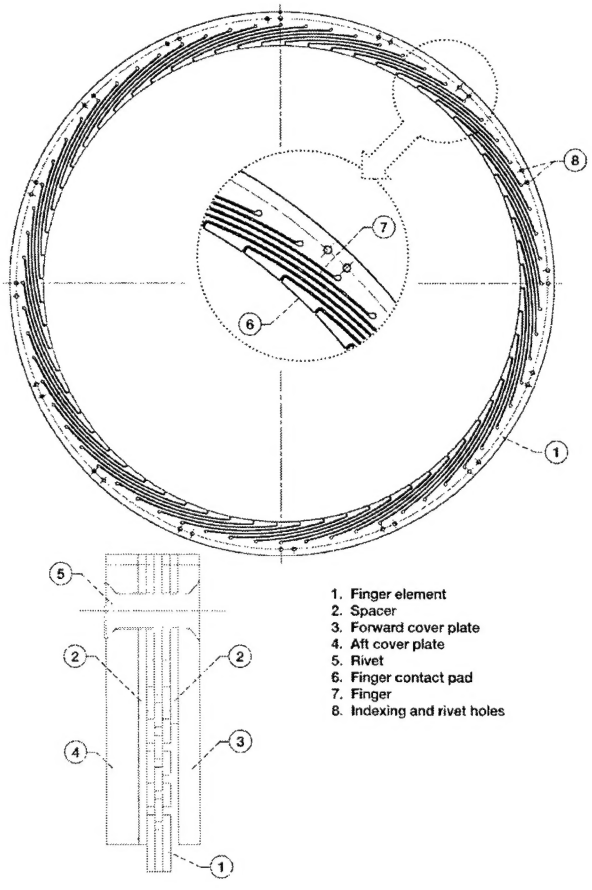

Figure 3.—Finger seal design.

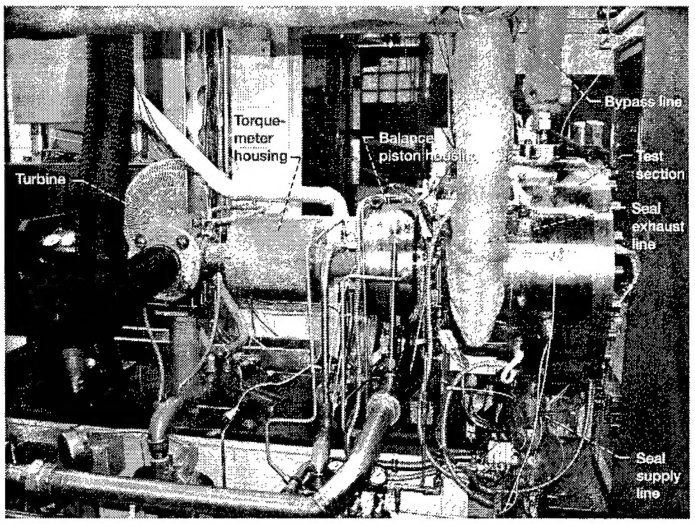

Figure 4.—High-temperature, high-speed turbine seal rig.

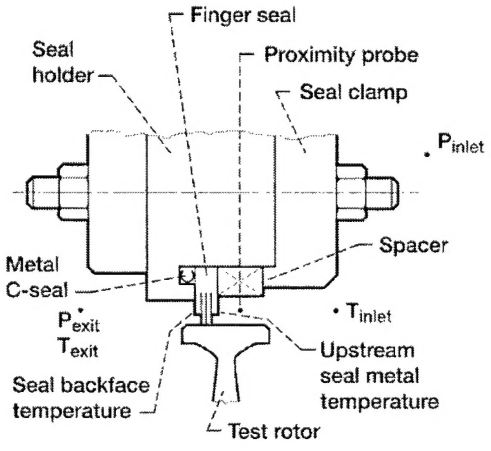

Figure 5.—Test seal configuration and location of research measurements.

Pitot tube-type flow meters are used to measure the flow rates of the hot air supplied to the rig and the air exiting the rig through the bypass line. The seal leakage rate is the difference between these two flow measurements. The seal leakage rate is then used to calculate the flow factor, which is defined as:

$$\phi = \frac{\dot{m}\sqrt{T_{avg}}}{P_u \times D_{seal}} \text{, kg-}\sqrt{\text{K}}\text{/MPa-m-s} \qquad (1)$$

The flow factor can be used to compare the leakage performance of seals with different diameters and with different operating conditions. The accuracy of the measured flow factor is ±1.5%.

A phase shift torquemeter measures the total torque of the seal test rig and compensates for any relative motion between the torsion shaft and stator. The torquemeter is rated to 22 N-m, has a maximum operating speed of 5236 rad/s, and an absolute accuracy of 0.13% or 0.028 N-m. The calculated seal torque is the measured rig torque with the test seal installed minus the rig tare torque. The rig tare torque was measured at various inlet air temperatures and speeds with no seal installed. This data was two-dimensionally curve fitted. The fitted curve is used with the measured average inlet air temperature and speed to infer the corresponding tare torque. Seal power loss is calculated as the seal torque multiplied by speed. The maximum error in the seal power loss measurements is 97.7 W over the range of test conditions. The speed measurement from the torquemeter is accurate to <0.04% or 1.4 rad/s at the maximum speed tested.

TEST PROCEDURES

Pre-test photographs were taken of all seals and rotors. Additionally, the seals were weighed and the rotor surface profile was recorded using a Talysurf profilometer.

Labyrinth seal tests were limited to static tests (no rotation) at room temperature where the pressure differential across the seal was increased to 483 kPa and back down to zero psid in 69 kPa increments. At each pressure differential, approximately 10 seconds of leakage data was recorded.

Four tests were conducted on both the brush seal and on the finger seal: a static leakage test, a performance test, an endurance test, and a post-endurance performance test. A final static test was also conducted on the brush seal. The conditions at which data were taken in these tests are shown in table 2. At each test condition data were recorded every second for approximately 10 seconds for the brush seal and 30 seconds for the finger seal.

In the static tests, the inlet air temperature was set and, for the brush seal, the pressure differential increased in 34.5 kPa increments to 517 kPa (or the maximum attainable pressure differential across the seal) and then decreased to 0 kPa in 34.5 kPa decrements. For the finger seal, 13.8 kPa increments were used between 0 and 207 kPa and 34.5 kPa increments were used between 207 and 517 kPa. At each condition seal leakage data were recorded. This procedure was repeated at each temperature.

Seal performance test data were taken at constant average seal inlet temperatures, pressure differentials across the seal, and surface speeds. At each average seal inlet temperature the pressure differential was set constant and surface speed was stepped up and down, taking data at each step. The seal inlet temperature was changed after obtaining data at all pressure and speed combinations. After the performance test, the seal and rotor were inspected and re-installed.

The endurance test measured seal performance over time at the highest temperature, pressure, and speed combination: 922 K, 517 kPa, and 366 m/s. The seal and rotor were removed for inspection after 1, 2, and 4 hours total test time. Both performance and static tests were then repeated for the brush seal. For the finger seal, only the performance test was repeated.

Table 2.—Brush and finger seal test matrices.

Seal	Test Type	Temp., K	Pressure, kPa	Speed, m/s
Brush	Static	294, 533, 700, 811, 922	0 - 517 - 0	0
Brush	Performance	294, 533, 700, 811, 922	69, 276, 517	0, 183, 274, 366, 274, 183, 0
Brush	Endurance	922	517	366
Brush	Post-endurance Performance	294, 533, 700, 811, 922	69, 276, 517	0, 183, 274, 366, 274, 183, 0
Brush	Static	294, 533, 700, 811, 922	0 - 517 - 0	0
Finger	Static	294, 700, 922	0 – 517 - 0	0
Finger	Performance	700, 866, 922	69, 276, 517	0, 183, 274, 366, 274, 183, 0
Finger	Endurance	922	517	366
Finger	Post-endurance Performance	700, 866, 922	69, 276, 517	0, 183, 274, 366, 274, 183, 0

For each inspection the seal and test rotor were first visually inspected. Then the seal was weighed and its average inner diameter was measured. The overall seal and a close-up view of the seal bristles or fingers were photographed. Rotor wear was quantified using a profilometer. Eight measurements were taken around the circumference of the rotor to determine an average track width and depth. Photographs of the overall rotor and close-ups of the rotor coating were also taken.

LEAKAGE PERFORMANCE

Initial Static Test

Room Temperature. Brush seal and labyrinth seal leakage performance at static, room temperature conditions is shown in figure 6 as flow factor versus pressure differential across the seal. The brush seal's flow factor is greater while increasing pressure differential than while decreasing

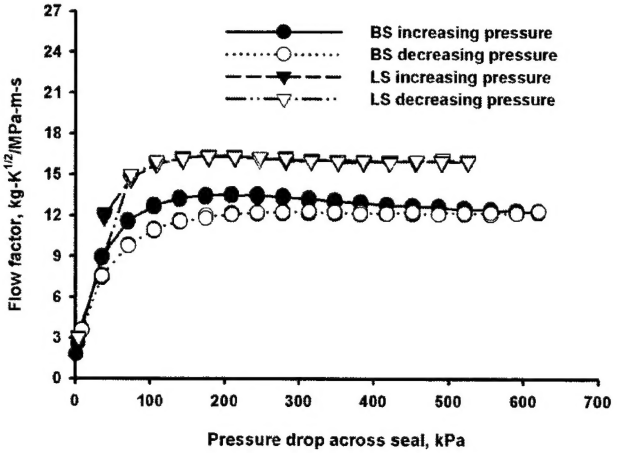

Figure 6.—Static leakage performance of brush seal (BS) and labyrinth seal (LS) at average seal inlet air temperature of 297 K.

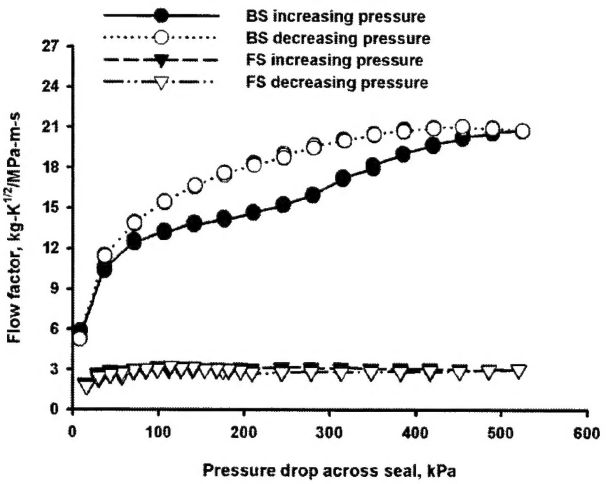

Figure 7.—Static leakage performance of brush seal (BS) and finger seal (FS) at average seal inlet air temperature of 922 K.

pressure differential due to the initial application of pressure seating the seal bristles. Flow factor increases until about 207 kPa where the flow chokes and the flow factor levels out to 12.2 kg-√K/MPa-m-s. Assuming isentropic, compressible, choked flow through an annular clearance with an inner diameter D_{seal}, the equivalent radial clearance of the brush seal is 96.5 μm. The maximum pressure drop attained was 621 kPa.

The labyrinth seal flow factor was the same for increasing pressure differential and decreasing pressure differential. The flow factor increases until about 103 kPa where it levels out to about 16.0 kg-√K/MPa-m-s and the flow chokes. This is 91% of the predicted flow factor of 17.6 kg-√K/MPa-m-s calculated using the KTK code. The maximum pressure differential attained was 524 kPa.

The static leakage flow factor at room temperature of the brush seal with an initial radial interference of 96.5 μm is 24% less than the 4-knife labyrinth seal with a 229 μm radial clearance. The equivalent radial clearance for the brush seal is, coincidentally, 96.5 μm. The lower leakage of the brush seal is accomplished with a seal of 4.27 mm total axial length compared to the 4-knife labyrinth seal which has an axial length of 11.2 mm. Hence the brush seal leakage is 24% less than the labyrinth seal and uses only 38% of the axial space the labyrinth seal requires. It is anticipated that for operation at temperatures to 922 K and surface speeds to 366 m/s that the labyrinth seal would require a 305 μm radial clearance at build to avoid a rub with the rotor. The predicted leakage flow factor for a labyrinth seal with a 305 μm radial clearance is approximately 25 kg-√K/MPa-m-s, which is two times greater than that measured for the brush seal.

922 K. Brush and finger seal leakage performance at 0 rpm and 922 K average seal inlet air temperature are compared in figure 7. The brush seal exhibits an unusual behavior as the pressure drop increases in that the flow factor initially starts to level off around 69-103 kPa, but then starts increasing again at 276 kPa until it levels off at 414 kPa. This trend corresponds to changes in the average seal inlet air temperature during the test. As the pressure drop decreases the flow factor remains at a higher level and it appears the flow is choked at 379 kPa at a flow factor of 21.2 kg-√K/MPa-m-s. A maximum pressure differential of 525 kPa was obtained. Assuming isentropic, compressible, choked flow, the equivalent radial clearance of the brush seal at 922 K changed from 109 μm at 138 kPa to 165 μm at 489 kPa as the pressure differential was increased. As pressure differential decreased the equivalent clearance remained at about 165 μm.

The finger seal flow factor increases with pressure drop until about 103.4 kPa and then levels off at a flow factor of approximately 2.89 kg-√K/MPa-m-s. At this point the flow is choked [6]. The flow factor of the finger seal is 14% of the flow factor of the brush seal for this 922 K static test. This is unusual compared to previous tests with 129.5 mm seals [3,4] which indicated that brush and finger seal leakage performance was similar. This difference in performance may be due to the brush seal having about half the initial interference with the rotor than the finger seal. Also, at 922 K the radial interference between the bristles and the rotor is reduced to 12.7 μm due to the difference between the coefficient of thermal expansion (CTE) for the Mar M-247 rotor and the Haynes 25 bristles. Additionally, there had been no shaft rotation, which facilitates the bristles to move to their optimum positions.

The four-knife labyrinth seal with a 305 μm radial clearance at room temperature will have a 394 μm radial clearance at 922 K due to thermal expansion and the different coefficients of thermal expansion for the Inconel 625 seal and the Mar M-247 rotor. At this clearance the labyrinth seal has a predicted flow factor of 33.8 kg-√K/MPa-m-s, which is 1.6 times greater than the measured flow factor of the brush seal and 11.7 times greater than the finger seal.

Performance Test

700 K. The leakage performance of the brush seal at an average seal inlet air temperature of 700 K at pressure differentials of 69, 276, 517 kPa is shown in figure 8. For all

pressure differentials the flow factor decreases as speed increases due to centrifugal growth of the rotor, which decreases the seal clearance. At 69 kPa there is a large hysteresis where the flow factor for increasing speed is higher than for decreasing speed. However, this observation is contrary to what happens if the bristles get stuck on the backplate. Hysteresis may occur when speed increases and the centrifugal growth of the rotor pushes the bristles or fingers radially away. When the speed decreases and the rotor diameter shrinks, the bristles or fingers may remain in their outer position causing leakage and flow factor to increase. Hysteresis may also be due to radial wear of the seal during initial shaft rotation, which would increase the seal clearance. Likewise, seal holder and rotor temperature changes can affect the seal clearance and appear as hysteresis. It is likely, however, that the high flow factor while speed was increasing at 69 kPa relative to decreasing speed is evidence that the bristles are moving to their optimum position at this temperature. At 276 and 517 kPa small hysteresis is exhibited and it is more typical with the flow factor being less while speed is increasing than when speed is decreasing. Also, the flow factors at 276 and 517 kPa are about the same. At the maximum speed tested, 366 m/s, the flow factor is approximately 5.72 $\pm$ 0.21 kg-$\sqrt{K}$/MPa-m-s. At 0 rpm, 517 kPa the average flow factor is about 16.37 kg-$\sqrt{K}$/MPa-m-s.

Finger seal leakage performance at 700 K is shown in figure 9. Overall, the finger seal flow factor at 69 kPa is less than at 276 and 517 kPa. Also, the flow factor data at 69 kPa and for increasing speed at 276 and 517 kPa are about the same, approximately 3.1 to 3.5 kg-$\sqrt{K}$/MPa-m-s. Hysteresis can be seen in the data taken at 276 and 517 kPa and is more pronounced at 517 kPa. The flow factor is low however, with a maximum of 9.14 kg-$\sqrt{K}$/MPa-m-s at 0 m/s and 517 kPa. The flow factor at 366 m/s is 4.689 $\pm$ 0.037 kg-$\sqrt{K}$/MPa-m-s.

The finger seal leakage performance at 700 K was significantly better than the brush seal. Flow factor for the finger seal was about 60% of that for the brush seal at 0 m/s and 517 kPa and about 75% of the brush seal at 366 m/s. The 305 μm radial clearance labyrinth seal will have a radial clearance of 254 μm at 700 K and 366 m/s and a predicted flow factor of 28.2 kg-$\sqrt{K}$/MPa-m-s. This is 4.9 times greater than the brush seal and 6 times greater than the finger seal at these conditions.

922 K. The brush seal leakage performance at 922 K is shown in figure 10. For 69, 276, and 517 kPa, the flow factor decreases as speed increases due to centrifugal growth of the rotor. The flow factors for increasing speed are greater than for decreasing speed. Again this is contrary to what is usually observed during performance tests for brush seals. It is possible that as the speed is first increased at each pressure the vibration of the rotor helps to work the bristles into their optimum position. For the decreasing speed data, flow factor increases with increased pressure differential, except at 0 rpm. At 366 m/s, the average flow factor is 6.96 $\pm$ 0.43 kg-$\sqrt{K}$/MPa-m-s. At 0 rpm and 517 kPa, the flow factor is 21.046 $\pm$ 0.252 kg-$\sqrt{K}$/MPa-m-s.

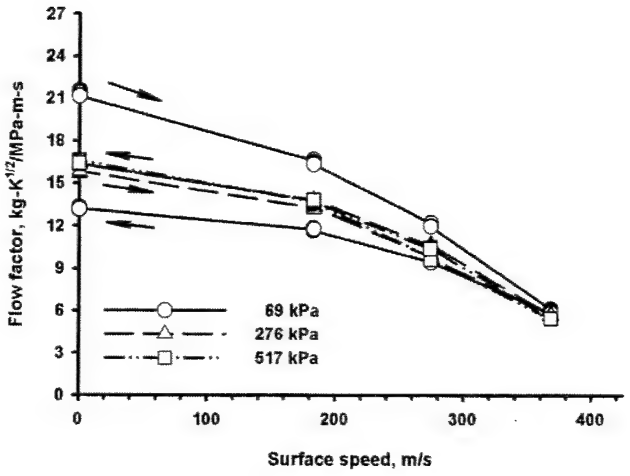

Figure 8.—Brush seal performance test data at 700 K average seal inlet air temperature and 69, 276, and 517 kPa pressure drops across seal.

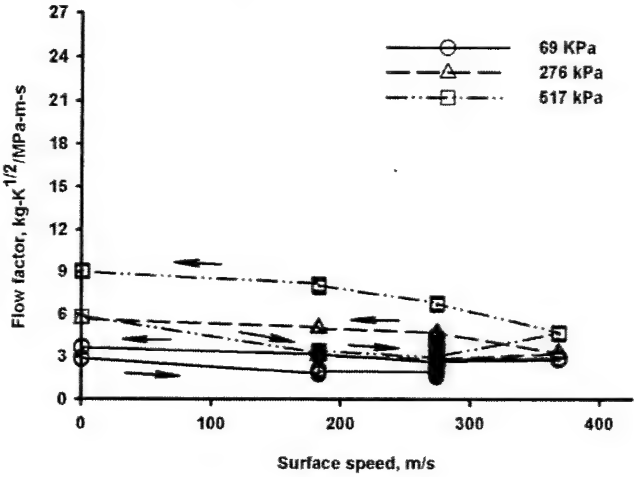

Figure 9.—Finger seal (FS) performance test data at 700 K average seal inlet air temperature and 69, 276, and 517 kPa pressure drops across seal.

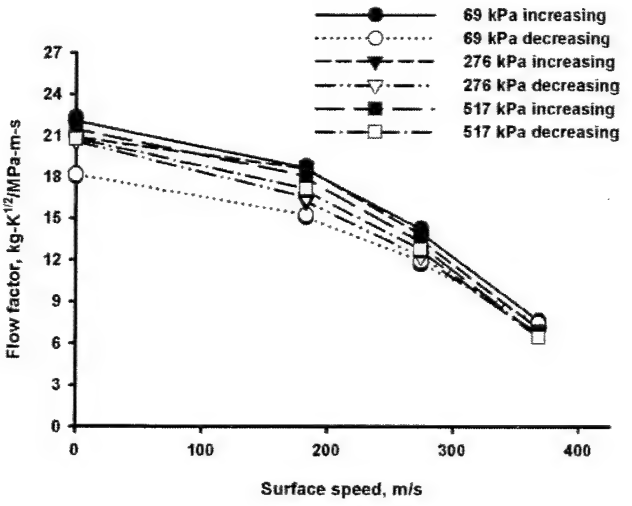

Figure 10.—Brush seal performance test data at 922 K average seal inlet air temperature and 69, 276, and 517 kPa pressure drops across seal.

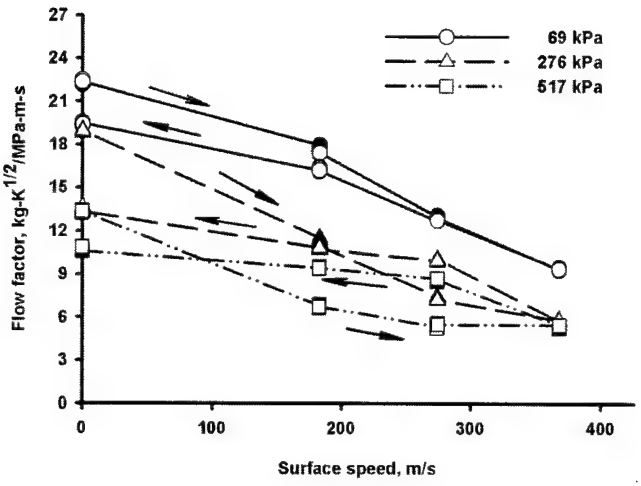

Figure 11.—Finger seal performance test data at 922 K average seal inlet air temperature and 69, 276, and 517 kPa pressure drops across seal.

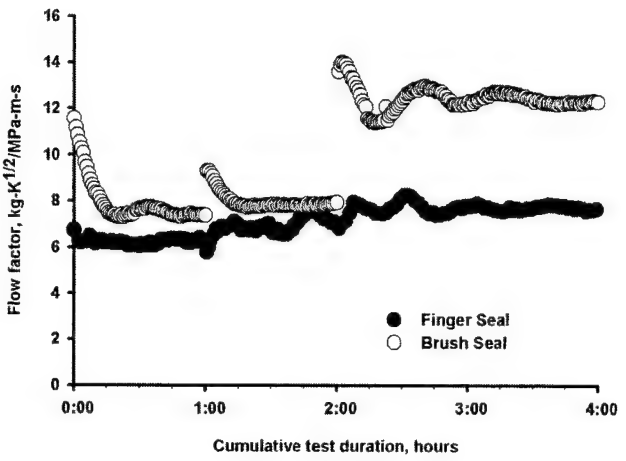

Figure 12.—Time history of finger seal (FS) and brush seal (BS) endurance tests at 922 K average seal inlet air temperature, 366 m/s surface speed, and 517 kPa pressure drop across seal.

The finger seal leakage performance at 922 K is shown in figure 11. As expected, at all three pressure differentials flow factor decreases as speed increases due to centrifugal growth of the rotor reducing the clearance. Hysteresis is evident for all three pressure differentials tested and may be due to changes in the clearance between the seal holder and the rotor and not due to the fingers getting stuck in the open position [6]. Also, for all three pressure differentials tested, the flow factor at 366 m/s is between 5.532 – 9.418 kg-√K/MPa-m-s. At 0 rpm and 517 kPa, the flow factor ranges from 10.778 to 13.324 kg-√K/MPa-m-s.

The brush seal and finger seal leakage performance data are similar in that as speed increases, flow factor decreases due to centrifugal rotor growth reducing the seal clearance. The flow factor of the finger seal at 69 kPa is very similar to the brush seal at all three pressure differentials. At 517 kPa the finger seal flow factor is about half that of the brush seal at speeds between 0 and 274 m/s. However at 517 kPa and 366 m/s the finger seal flow factor is only slightly less than the brush seal flow factor. At 922 K and 366 m/s the four-knife labyrinth seal would have a radial clearance of 312 μm and a predicted flow factor of 26.1 kg-√K/MPa-m-s. This is 3.75 times larger than the brush seal data and 2.8 to 4.75 times greater than the finger seal data.

Endurance Test. Brush seal and finger seal performance during the 4 hour endurance test is shown in figure 12. During the first hour the brush seal flow factor leveled out to 7.14 to 7.82 kg-√K/MPa-m-s and during the second hour the flow factor leveled out to 7.72 to 8.11 kg-√K/MPa-m-s, a slight increase. During the third and fourth hours the brush seal flow factor was about 62.5% higher than during the first 2 hours and at the end of the endurance test the flow factor was 12.06 kg-√K/MPa-m-s. The calculated isentropic choked flow equivalent clearance for the brush seal increased from 61 μm to 97 μm between the second hour and the third and fourth hours. It is also interesting to note that on each day of the test the brush seal flow factor decreased over the first quarter hour. Higher temperatures existed during the third and fourth hours compared to the second hour of the brush seal test suggesting that the radial clearance increased between the seal and the rotor. The average seal inlet air temperature was approximately 14 K higher during hours 3 and 4 than during the second hour of the endurance test. Also, the seal holder temperature at the 180° location was 55 K higher during hours 3 and 4 than during the second hour of the endurance test. A higher seal holder temperature would tend to increase the seal clearance.

The flow factor for the finger seal endurance test increased from about 6.37 kg-√K/MPa-m-s at the beginning to about 7.72 kg-√K/MPa-m-s at the test end. The equivalent radial clearance of the finger seal during the endurance test was 61 μm. At the end of the endurance test the finger seal had a flow factor 36% less than the brush seal. This could be because the brush seal started with a smaller amount of radial interference than the finger seal. A labyrinth seal with an initial room temperature, static radial clearance of 305 μm would have a predicted clearance at 922 K, 366 m/s of 312.4 μm and a predicted flow factor of 26.1 kg-√K/MPa-m-s. This is 2.16 and 3.38 times higher than the brush and finger seal at test end, respectively.

Post-endurance Performance Test. The post-endurance performance test results of the brush and finger seals are shown in figure 13. The brush seal flow factor at 922 K, 366 m/s, and 517 kPa for the post-endurance performance test was 17.37 kg-√K/MPa-m-s, which is 2.5 times greater than the initial performance test at those conditions. The finger seal post-endurance performance test flow factor at 922 K, 366 m/s and 517 kPa was 1.6 times greater than during the initial performance test. The flow factor for the brush seal increased more than for the finger seal probably because the brush seal had less initial interference. The finger seal flow factor decreases with increased pressure differential, indicating a definite pressure closing effect. The brush seal flow factors show less dependence on the differential pressure across the seal than the finger seal.

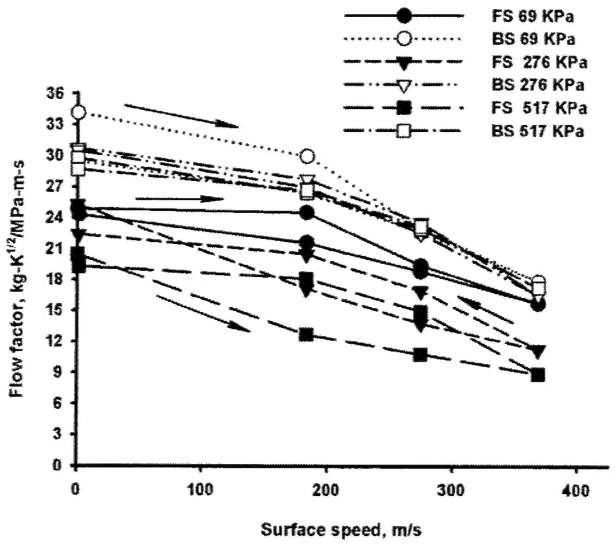

Figure 13.—Post-endurance performance test. Finger seal and brush seal average flow factor versus average surface speed at 922 K average seal inlet air temperature and 69, 276, and 517 kPa pressure drop across seal.

POWER LOSS

The power loss of the brush seal at 297 K, fig. 14, shows the initial power loss as the brush seal is being worn. Note that at 69 kPa, 183 m/s for increasing speed that the power loss is nearly the same as for 517 kPa. From that point the power loss decreases as the speed increases to 366 m/s. Then as the speed decreases back to 0 m/s, the seal power loss is reduced to about 186 W. After the brush seal is worn the seal power loss curves become very consistent and repeatable with only very slight decreases in power loss over time. The curves take an expected shape with seal power loss increasing with increasing speed and with higher power loss at higher pressure differential across the seal, since the pressure differential results in a net closing force on the bristles. This seal power loss data indicates that there is a well defined relationship between pressure differential and pressure closing effect on the bristles. The maximum brush seal power loss occurs at 297 K, 517 kPa, and 366 m/s and has a value of 10.4 kW.

The brush seal and finger seal power loss at an average seal inlet temperature of 922 K are compared in figure 15 as a function of surface speed for 69, 276, and 517 kPa pressure differential across the seal. Previously it was shown that the brush and finger seal data were in excellent agreement [6]. The power loss for the brush seal in figure 15 is for a different brush seal of the same design as that presented in reference 6. The trends of the brush and finger seal power loss are very similar. The brush seal has a maximum power loss at 922 K, 366 m/s and 517 kPa of 9.97 kW. The finger seal has a power loss of 9.38 kW at the same conditions. The power loss for the finger seal is slightly less than for the brush seal.

The post-endurance performance test brush and finger seal power loss are compared in figure 16 and again the finger seal power loss is less than the brush seal power loss. However, there is a greater difference between the finger and brush seal power loss in the post-endurance

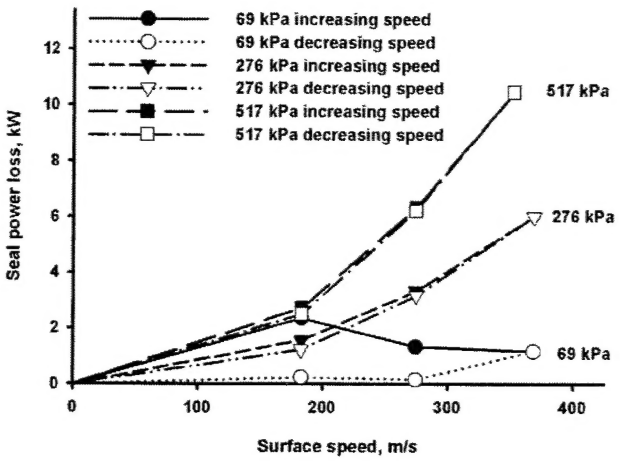

Figure 14.—Brush seal average power loss versus average surface speed at 297 K average seal inlet air temperature and 69, 276, and 517 kPa pressure drop across seal.

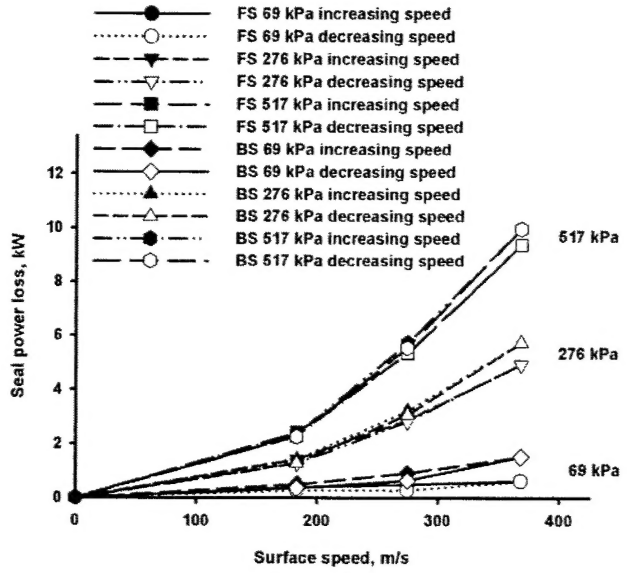

Figure 15.—Performance test. Finger seal (FS) and brush seal (BS) average power loss versus average surface speed at 922 K average seal inlet air temperature and 69, 276, and 517 kPa pressure drop across seal.

performance test than in the first performance test. In comparing the finger seal power loss in figure 15 and figure 16, there is no observable change in the power loss at 69 and 276 kPa, but only at 517 kPa where the post-endurance performance test finger seal power loss is slightly greater. The final seal power loss for the finger and brush seal at 922 K, 366 m/s and 517 kPa are 9.72 and 10.48 kW, respectively.

The authors recognize that the seal power loss values presented in figures 14, 15, and 16 may be substantially higher than the true seal power loss since the tare torque was measured at ambient pressure. However, the data presented still provide insight to the seal behavior and the comparisons between the finger seal and the brush seal are still valid. When a pressure differential is applied to the seal the windage from the high pressure side of the test

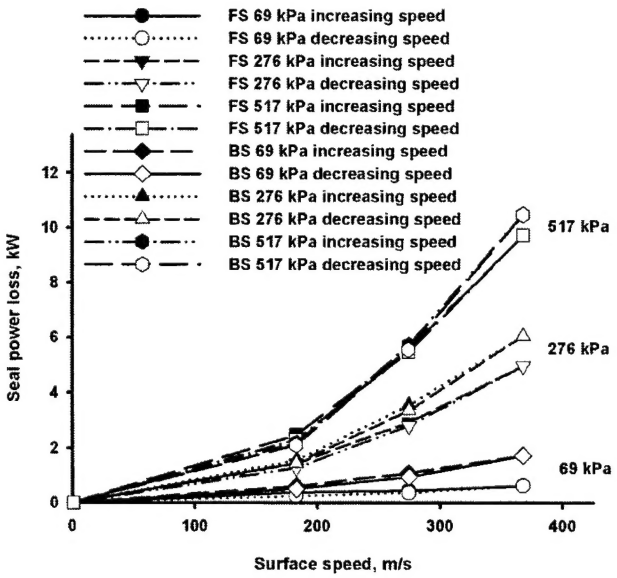

Figure 16.—Post-endurance performance test. Finger seal (FS) and brush seal (BS) average power loss versus average surface speed at 922 K average seal inlet air temperature and 69, 276, and 517 kPa pressure drop across seal.

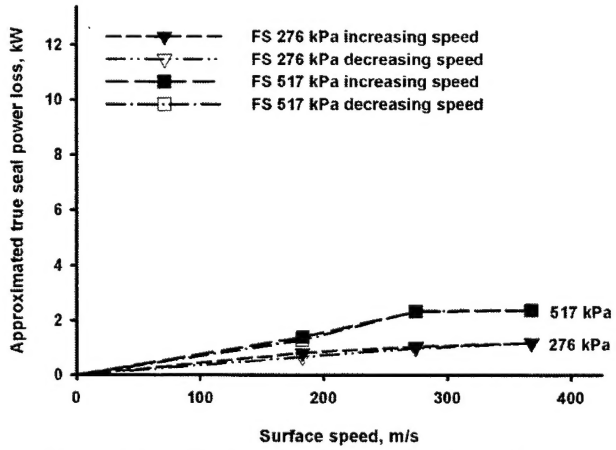

Figure 17.—Performance test. Finger seal (FS) approximated true average power loss versus average surface speed at 922 K average seal inlet air temperature and 276 and 517 kPa pressure drop across seal.

rotor and the balance piston increases due to the density of the air. In addition, the test end bearing experiences an additional axial load of 1334 N, which will increase the bearing windage beyond what is included in the measured tare torque. Windage error in the tare torque due to changes in oil viscosity is expected to be small since the bearing temperature variation between the seal tests and the tare test was very small.

An approximation of the additional windage on the high pressure side of the test rotor and balance piston was made using an approximate solution provided by Schlichting [7]. The additional torque from the higher axial load on the test end bearing was estimated using a friction coefficient of 0.0015 in the equation [8] below:

$$T = f D_1 W/2 \qquad (2)$$

These approximated additional tare losses were subtracted from the finger seal power loss data of figure 15 and the approximated true seal power loss of the finger seal is shown in figure 17. The approximated true seal power loss increases with speed and with pressure differential. At 69 kPa, the approximated true seal power loss was negligible. The maximum approximated true seal power loss of 2.36 kW occurs at 517 kPa and 366 m/s. This is 4 times less than the maximum finger seal power loss obtained using the measured tare torque with no pressure differential across the test and balance piston rotors. Hence, this finding suggests that additional testing with a straight cylindrical seal and/or a labyrinth seal is needed to establish tare torque data that accounts for pressure differentials across the test seal. Also, further investigation is needed to explain why the approximated true seal power loss at 517 kPa leveled out at higher speeds.

Other approaches to measure seal power loss were considered before deciding to install a torquemeter in the test facility. One approach was to simply measure the seal leakage rate and the seal inlet and exit air temperatures and assume the seal operates in an adiabatic environment and that all the frictional heating goes into the seal leakage flow. Then one could simply calculate the seal power loss as mass flowrate multiplied by specific heat and the temperature change. However, it has been observed in testing that the seal exit air temperatures were invariably lower than the seal inlet air temperatures and hence the seal power loss would be negative. In reality, the thermocouples measuring the seal inlet and exit air temperatures are about 7 to 10 cm away from the seal, labyrinth seal purge air mixes with the seal leakage in the exhaust cavity, radiant and conductive heaters in the test section make the seal environment anything but adiabatic, and there are conductive heat transfer paths from the seal to the rotor and from the seal to the seal holder. Building a thermal model of the seal test section and using the available leakage, temperature, and pressure measurements to back out the seal power loss was considered, but soon dismissed after considering the uncertainties of all the assumptions required to build the model. It was decided that measuring torque would produce more reliable results.

If valid friction coefficients and contact pressures were available, one could calculate the frictional seal power loss for the finger or brush seal as

$$P_{ower} = \mu \cdot P \cdot A \cdot U \qquad (3)$$

In addition to the specific design features of the seal that control the bristle pack or finger stiffness, the contact pressure will be influenced by the initial interference, pressure differential across the seal, centrifugal growth of the rotor, and the relative coefficient of thermal expansion of the seal, seal holder, and test rotor and their actual temperatures. This approach is provided for the reader to pursue if interested.

WEAR PERFORMANCE

Seal wear

The brush seal and finger seal accumulative weight loss versus accumulative run time is shown in figure 18. The total weight loss from the brush seal was 0.967 g of which 71% was lost in the initial performance test. Using the bristle density at the seal inner diameter, bristle diameter and angle, material density, and measured weight loss the calculated expected change to the seal inner radius was 131 μm. This is in good agreement with the measured seal inner radius change of 140 μm between pre-test and after the performance test. Based on the measured weight loss, the brush seal has a final static, room temperature radial clearance of 34.5 μm.

The finger seal had a total weight loss of about 6 grams, which assuming the wear occurred uniformly around the seal circumference would yield a calculated radial wear of 889 μm, or slightly more than half the finger pad thickness. Over 70% of the finger seal weight loss also occurred during the initial performance test [6].

One can see that the brush seal weight loss was about one-sixth of the finger seal weight loss. Also, the calculated finger seal radial wear of 889 μm is 6.8 times larger than the calculated brush seal wear. This may in part be explained by the fact that the finger seal had a larger initial radial interference with the rotor than the brush seal (165.1 μm for the finger seal and 96.5 μm for the brush seal). Based on the measured weight loss, the finger seal had a final static, room temperature radial clearance of 723.9 μm, which is 21 times greater than the final brush seal clearance.

Rotor wear

Rotor wear was quantified using a profilometer. Eight measurements were taken around the circumference of the rotor to determine an average track width and depth. These averages for the track created by the finger seal are presented in table 3 for each inspection. Rotor wear due to the brush seal was very minimal.

Table 3.—Average rotor wear track measurements for finger seal.

Seal:	Finger	Finger
Test type	Width, μm	Depth, μm
Baseline	0	0
Performance	2413	6.22
First hr endurance	2108	4.47
Second hr endurance	2642	4.19
Fourth hr endurance	2413	6.32
Last Performance	2438	5.49

For the finger seal, both the track width and depth measurements indicate that the majority of the seal wear took place during the first performance test. The average track width ranged from 2 to 2.54 mm and the average track depth ranged from 3.8 to 6.4 μm. This is a small and acceptable amount of wear. The scatter in the data is likely due to the uncertainty in taking the measurements at the same circumferential location on the rotor for each inspection. The circumferential locations were visually sighted using the bolt hole locations and etch marks as guides. Given that the performance test effectively covers the entire range of temperatures, pressures and surface speeds to which the seal would be subjected, it is likely that the overall seal track width was worn in during this first performance test.

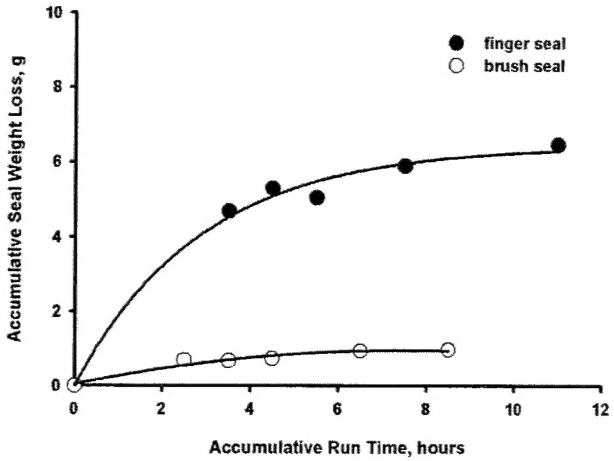

Figure 18.—Finger seal (FS) and brush seal (BS) accumulative weight loss versus accumulative run time.

CONCLUSIONS

Based on the results of testing a 229 μm radial clearance 4-knife labyrinth seal at room temperature, static conditions; predicting leakage performance for a 305 μm radial clearance 4-knife labyrinth seal at high temperatures and speeds; and testing a brush seal and a finger seal at inlet air temperatures to 922 K, surface speeds to 366 m/s and pressure differentials to 517 kPa the following conclusions are made:

1. At room temperature, static conditions a brush seal with a 96.5 μm radial interference leaks 24% less than a 4-knife labyrinth seal with a 229 μm radial clearance and uses only 38% of the axial space that the labyrinth seal requires.
2. At 922 K, initial static conditions the finger seal flow factor is 14% of the brush seal flow factor, which is counter to previous test results [3,4]. This may be due to the brush seal having about half the radial interference (at room temperature) as the finger seal and a near loss of interference at 922 K due to different coefficients of thermal expansion for the rotor and brush seal materials.
3. In the 700 K performance test, the finger seal flow factor was 60 to 75% of the brush seal flow factor.
4. In the performance test at the maximum test condition of 922 K, 517 kPa, and 366 m/s the finger seal flow factor of 5.5 kg-$\sqrt{K}$/MPa-m-s was only slightly less than the brush seal flow factor of 6.96 kg-$\sqrt{K}$/MPa-m-s.
5. Overall the finger seal that was tested had a lower flow factor during the endurance test than the brush seal.

Although the difference was small during the first two hours of the test, after 4 hours the finger seal flow factor was 36% less than the brush seal flow factor.

6. The 229 μm radial clearance of the labyrinth seal is too small to safely use during rotation. Predicted flow factor for a labyrinth seal at 922 K, 366 m/s and 517 kPa with a 305 μm radial clearance at build is 2.2 and 3.38 times larger than the flow factor measured at the end of the endurance test for the brush seal and finger seal, respectively. Hence, both the brush and finger seal offer substantial improvements in leakage performance over labyrinth seals.
7. The finger seal exhibited a more pronounced pressure closing effect than the brush seal.
8. The finger and brush seals have very similar power losses. At 922 K, 366 m/s, 517 kPa the finger and brush seal power loss was 9.72 and 10.48 kW, respectively, based on tare data with zero pressure difference across the test rotor. Since the approximated true power loss for the finger seal at the same conditions is four times less, additional testing with a straight cylindrical or labyrinth seal is needed to establish tare torque data that accounts for the pressure difference across the test rotor and balance piston.
9. Wear of the chrome carbide rotor coating was minimal. The majority of the seal wear occurred during the initial performance test for both the brush and finger seals. The brush seal had an initial build radial interference of 96.5 μm and wore radially 131 μm, thus the final static room temperature radial clearance of the brush seal was 34.5 μm. The finger seal had an initial build interference of 165 μm and wore radially 889 μm, thus the final static room temperature radial clearance was 724 μm or 21 times greater than the brush seal.

REFERENCES

[1] Steinetz, B. M., and Hendricks, R. C., 1997, "Engine Seals." *Tribology for Aerospace Applications,* E.V. Zaretsky, ed., Society of Tribologists and Lubrication Engineers, Park Ridge, IL, pp. 595–682.

[2] Mechanical Technology Inc., Chupp, R. E., Holle, G. F., and Scott, T. E., 2003, User's Manual for the Labyrinth Seal Design Model, NASA CR-212367. Available from the NASA Center for Aerospace Information.

[3] Arora, G. K., and Proctor, M. P., 1997, "JTAGG II Brush Seal Test Results," NASA TM 107448, AIAA–97–2632, ARL–TR–1397.

[4] Arora, G.K., Proctor, M. P., Steinetz, B.M., and Delgado, I.R., 1999, "Pressure Balanced, Low Hysteresis, Finger Seal Test Results," NASA TM—1999-209191, ARL–MR–457, AIAA–99–2686.

[5] Arora, G. K., and Glick, D. I., 2001, "Pressure Balanced Finger Seal," U. S. Patent 6,196,550.

[6] Proctor, M. P., Kumar, A., and Delgado, I.R., 2002, "High-Speed, High-Temperature Finger Seal Test Results," NASA/TM—2002-211589, ARL–TR–2781, AIAA–2002–3793.

[7] Schlichting, H., 1979, *Boundary Layer Theory, Seventh Edition,* McGraw-Hill, Inc., New York, pp. 242–243.

[8] Townsend, D.P., Editor in Chief, 1991, *Dudley's Gear Handbook, 2nd edition,* McGraw-Hill, Inc., New York, pp. 12.17–12.24.